

# Electromechanical Modelling and Stress Analysis of RF-MEMS Capacitive Shunt Switch

Gopichand Ch (✉ [gopichand515@gmail.com](mailto:gopichand515@gmail.com))

Mizoram University

Reshmi Maity

Mizoram University

K. Srinivasarao

Koneru Lakshmaiah University

N.P. Maity

Mizoram University

K. Girija Sravani

National Institute of Technology Silchar

---

## Research Article

**Keywords:** RF MEMS shunt switch, Stress gradient, Perforations, Meanders

**Posted Date:** November 30th, 2021

**DOI:** <https://doi.org/10.21203/rs.3.rs-407210/v1>

**License:**  This work is licensed under a Creative Commons Attribution 4.0 International License.

[Read Full License](#)

---

# Electromechanical Modelling and Stress Analysis of RF-MEMS Capacitive Shunt Switch

Ch. Gopi chand<sup>1\*</sup>, Reshmi Maity<sup>1</sup>, K. Srinivasarao<sup>2</sup>, N.P. Maity<sup>1</sup>, K.Girija Sravani<sup>3</sup>

<sup>1</sup>Department of Electronics and Communication Engineering, Mizoram Central University, Aizwal, Mizoram, India.

<sup>2</sup>MEMS Research Center, Department of ECE, Koneru Lakshmaiah Education Foundation (Deemed to be university), Green Fields, Vaddeswaram, Guntur-522502, India.

<sup>3</sup>Department of Electronics and Communication Engineering, National Institute of Technology, Silchar, Assam, India

\*The Corresponding author E-mail address: gopichand515@gmail.com

**Abstract---** This paper presents the simulation and theoretically calculation results of a shunt switch with Electro-mechanical modelling and stress gradient characteristics. The analysis is done with three membrane structures such as plane beam, incorporated with and without perforations, and non-uniform meander type beam, these are simulated in the COMSOL Multi-physics tool. The various Modal analyses are carried out for different values of residual stress gradients such as different structures, materials, and beam thickness. These analyzes are described by the fact that higher stress gradient values are undesirable for switching. By analysing all the results we have observed that the stress analysis for a shows that non-uniform meandered switch experiences maximum stress of 35.6 MPa, and center deflection of 0.06 MPa/ $\mu\text{m}$ , the deformations of the beam which is the least among the considered switches.

**Keywords:** RF MEMS shunt switch, Stress gradient, Perforations, Meanders.

## 1 Introduction

MEMS (Microelectromechanical system) technology is the miniaturization of mechanical and electro-mechanical devices and structures, using micro-fabrication techniques. The critical area of MEMS technology is they also performs devices and techniques that have great potential to improve the performance of communications circuits and systems [1-3]. RF (Radio frequency) MEMS switch particularly enables the realization of micro-size mechanical switches embedded in electronics devices. These devices are the integration of several micro-components on a single chip to form a microsystem that can sense and control an environment. In the last decade, devices such as switches, voltage-driven capacitors, inductors, acoustic and mechanical resonators, all employing MEMS technology, have experienced tremendous growth, particularly in radio frequency (RF) applications [4-7]. Among these devices, RF MEMS switches are one of the most fundamental and important MEMS devices in the microwave range. The MEMS devices renew to

replace their macro-scale counterparts due to their miniature size, low cost, low power consumption, and possible integration with semiconductor integrated circuit (IC) technology.

In spite of, RF electronic devices have continuously needed switches that offer low losses in the downstate and give good isolation with large allowable signal and low control power [8, 9]. RF MEMS devices combine tunable inductors, switches, variable capacitors. [10-12]. The switch is one of the numerous essential MEMS elements of the microwave frequency, which can be used to merge or split electronic circuits or improve signal directions. [13]. An RF MEMS switch is an electronic component that can restrain the attachment and detachment of RF signals. By comparing with a solid-state switch, RF MEMS switch has a lot of advantages are power consumption, low actuation voltage, high linearity, and good isolation, which have been widely utilized in communication systems in the past decade. [14-16]. These switches now a days have tremendous potential for implementation in downstream and conventional power supplies as a replacement for existing switching technology, as well as the potential for extremely adaptable RF systems. [17]. RF MEMS switches have received more consideration due to their high isolation, less insertion loss, good linearity, and power consumption are very low compared to semiconductor switches. The RF MEMS switches are employed in many applications such as satellite and defense applications, RF instrument test equipment, base station telecommunications infrastructures. MEMS reliability is a top priority for developers as it is increasingly being used in several industrial divisions in the application of pressure sensors, inertial sensors, micro mirror arrays, inkjet printer heads, and RF MEMS switches. All of these devices have its own moment of limiting or falling, this is nothing more than a membrane voltage. The reliability and performance of a membrane depend on its design. The stress was analyzed for different types of membranes made of gold and aluminum. The Von Misses stress has to be analyzed after the design of each part, as it reveals

whether the material will withstand the maximum stress levels, or if it leads to destruction [18]. The six modal patterns are analyzed for a range of residual stress gradients for both

compressive and tensile. There is a wide variation of the modal frequency values depending on the nature and magnitude of the residual stress gradient [19]. The effective residual stress is measured and calculated to be about 3–15 MPa in the corrugated bridge and 30 MPa in the flat bridge. The intrinsic residual stress is about 30 MPa regardless of the various thickness of the membrane in the flat bridge [20]. The highest stress and the lowest stress have been applied to the spring and the membrane, respectively. Therefore, for reducing the stress in the switch a special notice should be given to the spring design it can be maintained that only the stress of few points of the spring gets to 25 MPa [21].

This paper is arranged as follows, In Section 2, the structure of the proposed switch with different membranes, and its description are discussed. In Section 3, results and discussions of a switch are shown, and we have studied Electromechanical model analysis of proposed switch with analytical formulas, and also various simulations of stress analysis with different beam structures, thickness, various materials, and its properties, and finally, the Section-4 gives the conclusion of the entire paper.

## 2 Structure of Proposed Switch-Membrane and its Description

The proposed switch is having a coplanar waveguide (CPW), and it is made in a shunt configuration, the substrate is at a height of 210  $\mu\text{m}$  above the CPW transmission line with a resistance of 50 ohms. This CPW line is placed above an insulating layer to reduce some leakages. A thin layer of insulator acts like a dielectric layer to help generate capacitance across the signal line.

The signal layer of Si<sub>3</sub>N<sub>4</sub> is used as a dielectric layer under the middle of the switching beam to avoid direct contact. The dielectric layer is entirely dependent on the pull-in voltage used to turn the RF signal on and off through the transmission line. The schematic diagram of the RF MEMS switch is shown in Figure. 1 below.

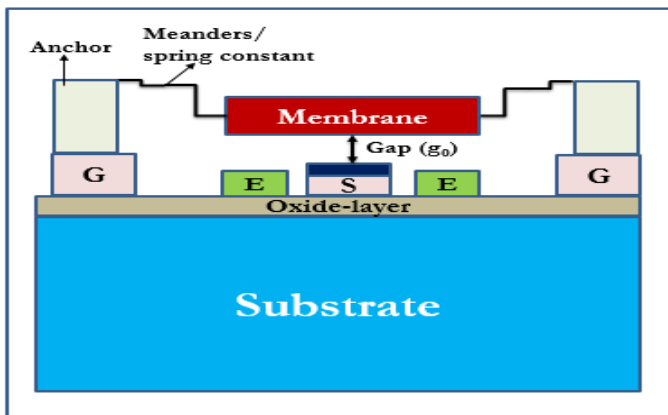


Fig. 1. Schematic view of RF-MEMS Shunt Switch

The authenticity of shunt switches is greatly influenced by dielectric charge and dielectric breakdown at high actuate voltages. The switching beam topology is critical to improving overall performance in terms of electromechanical and RF performance. Here are three types of switching diaphragms shown in Figures 2 and 3.

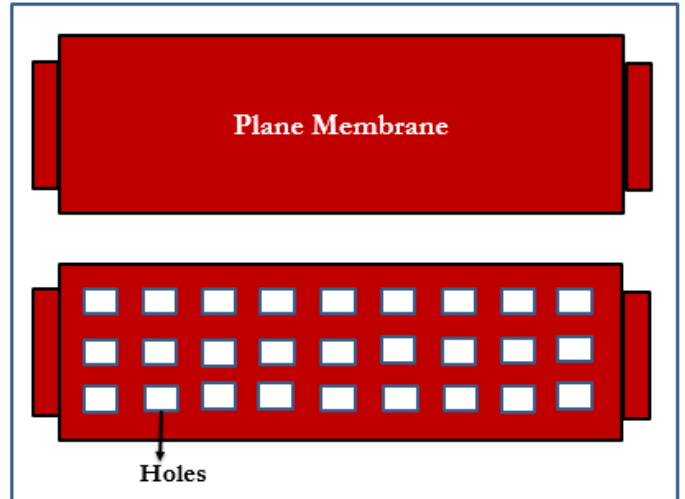


Fig. 2. Different membrane structure (with and without holes)

Meander helps to diminish the active Von Mises and lower the spring rate. Meanders that connect to the central layer help to decrease the bending of the middle membrane [22]. The actuating electrodes are located under this layer on both sides, so holes are provided to overcome the squeeze film damping and to enhance the switching speed. The perforation is directed towards the beam to reduce stiction and residual stress. The proposed meanders have a lower effective spring constant with the membrane. The holes are useful for reducing residual stress and Young's modulus of a device. Also, the appearance of holes creates a decrease in mass, which results in a higher mechanical resonance frequency. The proposed switch and its dimensions are described in Table 1.

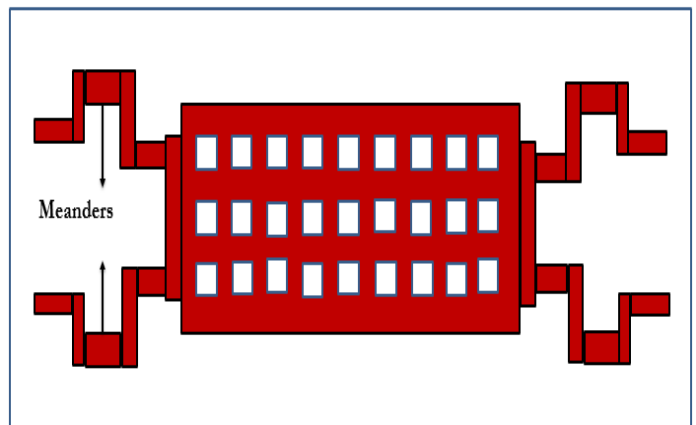


Fig. 3. Proposed beam structure of RF-MEMS Switch

$$kz = 0.5\epsilon_0 \frac{A}{(g-z)^2} V^2 \quad (4)$$

$$V = \sqrt{\frac{2kz(g-z)^2}{\epsilon_0 A}} \quad (5)$$

The derivative of the equation with respect to the beam height and setting that to zero, the height at which the change occurs is found to be exactly two-thirds of the zero-bias beam height, the final pull-in voltage formula is,

$$V_P = \sqrt{\frac{8Kg_0^3}{27\epsilon_0 A}} \quad (6)$$

Where, 'K' - stiffness of beam, 'g<sub>0</sub>' - gap, 'A' - actuation area, 'ε<sub>0</sub>' - permittivity of free space. The pull-in voltage is occurred as 1.9 V.

The spring constant (K) is a critical parameter in the mechanical design, the beam is created as a shunt configuration with four controllable ends. The spring stiffness for the controlled end of the membrane is determined by the equation, and it is schematically shown in Fig.4.

$$K = \frac{EWt^3}{l^3} \quad (7)$$

Where, 'E' - beam material elasticity, 'W', 't', and 'l' are width, thickness, and length respectively.

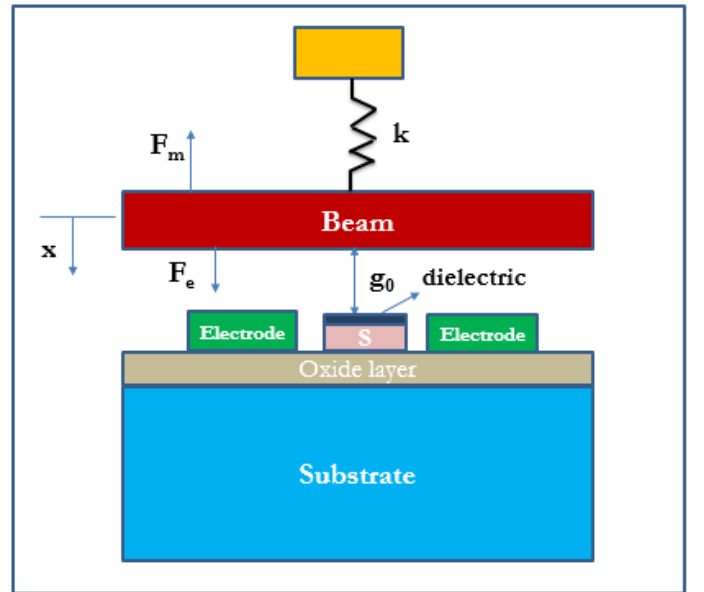


Fig. 4. Mechanical model schematic of RF-MEMS Switch

Table 1. Specifications of the proposed design

Sl. No	Structural Component	Length (μm)	Breadth (μm)	Height (μm)	Material
1	Substrate	820	300	210	Silicon
2	Ground	300	300	1	Gold
3	Oxide layer	820	300	2	Silicon dioxide
4	Beam	260	90	0.5	Gold
5	Signal line	100	300	1	Gold
6	Meander-1	20	10	0.5	Gold
7	Meander-2	35	1	0.5	Gold
8	Meander-3	30	10	0.5	Gold
9	Perforation	10	10	1	-----

### 3 Results and Discussions

#### 3.1.1 Electromechanical Model

The Electromechanical model and closed-form expression for a parallel plate capacitor is evaluated in this section. The Electrostatic actuation is caused by an electrostatic force acting on the capacitor plates under the applied voltage. Although the actual capacitance is more related to the fringing field, this model still presents a good opinion of electrostatic actuation [23]. The voltage is utilized, the membrane is actuated by an electrical field and to reach contact with a dielectric layer.

The capacitance of a fixed parallel plate capacitor is given by,

$$C = \epsilon_0 \frac{A}{(g-z)} \quad (1)$$

The energy stored 'W' in a capacitor with a voltage 'V', between the plates is given by equation,

$$W = 0.5\epsilon_0 \frac{A}{(g-z)} V^2 \quad (2)$$

The electrostatic force between the plates can be determined by differentiating the energy function for the coordinate in the direction of the force,

$$\frac{dW}{dz} = F = 0.5\epsilon_0 \frac{A}{(g-z)^2} V^2 \quad (3)$$

If the movable parallel plate is attached to a spring 'k', then under equilibrium condition,

The membrane is fixed between two anchors, there are having constant width and thickness. By utilizing the Euler–Bernoulli beam theory we have assume to verify the material is linearly elastic, the Poisson effect is neglected, and deformation of the beam. The Euler–Bernoulli beam theory results in the following equation,

$$EI \frac{d^2 z}{dx^2}(x) = M(x) \quad (8)$$

Here ‘E’ -Young modulus, ‘I’ - moment of inertia, ‘z(x)’ is the gap distance between the substrate and beam, and ‘M(x)’ is the bending moment at x location.

The derivative of the twisting moment, is given below,

$$\frac{dM}{dx}(x) = F_t(x) \quad (9)$$

The applied force of derivative is,

$$\frac{dF_t}{dx}(x) = f(x) \quad (10)$$

From equations 3 and 5, a relation can be assumed among z(x) and the electrostatic force per unit of length utilized to the beam  $f_e(x)$ , where the total force can be determined as,

$$EI \frac{d^4 z}{dx^4}(x) = f_e(x) \delta(x) \quad (11)$$

Here, ‘ $\delta(x)$ ’ signifies the appearance of the actuated electrode at ‘x’, location,

$$\delta(x) = \{1,0\} \quad (12)$$

Here, two conditions are denoted, such as the upper electrodes is mentioned by 1, if any is represented to zero.

The electrostatic force is given by,

$$f_e(x) = -\frac{1}{2} \frac{\epsilon_0 \omega V^2}{(z(x) + \frac{t_d}{\epsilon_d})^2} \quad (13)$$

Where ‘ $\epsilon_0$ ’ – permittivity of free space, ‘V’ is applied voltage, ‘ $t_d$ ’ is thickness of dielectric, and ‘ $\epsilon_d$ ’ is the relative permittivity. Finally, the overall equation of the scientific model is,

$$\frac{d^4 z}{dx^4}(x) = -\frac{1}{2EI} \frac{\epsilon_0 \omega V^2}{(z(x) + \frac{t_d}{\epsilon_d})^2} \delta(x) \quad (14)$$

When the membrane closes, the distribution of force and stress changes depending on the upward position. The membrane can no longer be modelled as a bridge with or without a clamp-clamp, but it is much more like a finite element plate resting on a set of point posts. A very high electrostatic force of ‘Fe’ acts on such a plate due to the small residual gap between the polysilicon electrode and the gold membrane. It is clear that for the maximum voltage value, the membrane tends to contract towards the electrode.

If the patterned ones are arranged in the form of a square with a side, the maximum displacement of the plate towards the electrode is,

$$\Delta_{dp} = 1.13 \frac{P_e}{E} \left( \frac{a_s^4}{t_b^3} \right) \quad (15)$$

It is mostly effected residual stress as,

$$P_e = \frac{F_e}{a_s^2} = \frac{1}{2} \frac{\epsilon_0 \omega_e l_e V_{bias}^2}{d_p^2 a_s^2} \quad (16)$$

Where ‘ $l_e$ ’ and ‘ $\omega_e$ ’ are the length and width of the electrode, respectively, and ‘ $V_{bias}$ ’ is the bias voltage applied to the suspension bridge.

### 3.1.2 Stress Analysis

The voltage level in the beam significantly influences the unwavering quality of the switch. In the event that the voltage is amazingly high, the switch will be harmed. In this, the stress level does not transcend the yield efficiency of the material. The reliability of the switch is depending on the stress level. Too much stress level is not good for the device, because it is easily breakdown and the membrane does not come back to its original position. Here, the electrostatic force is utilized between the beam and a transmission line. The voltage is applied on the two metal plates it will slightly under the step-down voltage, so the movable beam having maximum deflection. [24].

The stress is more concentrated on the edges of the fixed meanders. Here, the fixed edges are tightened, as the middle surface part of the beam is compressed, and we have observed that it can be functionally unloaded.

The influence of tensile and compressive stress gradients on a beam deflection due to applied displacement is described. The presence of perforation relieves stress in everything. The holes

are built into the beam, around which the voltage of the gaps is relieved. The critical stress was evaluated for the proposed switch using various beam materials. The significance of compressive stress that a membrane can withstand before buckling is called critical stress [25] it is calculated by,

$$\sigma_{cr} = \frac{\pi^2 Et^2}{3l^2(1-\nu)} \quad (17)$$

Where ‘E’ – Young’s modulus, ‘t’, and ‘l’ are thickness and length of the beam. The materials are to play a crucial role in the stress analysis, here, some materials and their properties are mentioned in the below Table.2.

**Table 2.** Various materials properties

Materials	Young’s Modulus (E)	Poisson’s Ratio (ν)
Aluminium (Al)	69	0.33
Copper (Cu)	125	0.36
Chromium (Cr)	140	0.2
Gold (Au)	79	0.42
Platinum (Pt)	177	0.39

The different metals such as aluminium, copper, chromium, gold, and platinum have been examined for designing the various beam structures. We have analyzed the average stress of gold in each membrane with beam thickness of 0.5 μm, it shows good results by comparing with other materials as shown in Figs.5, 6, and 7.

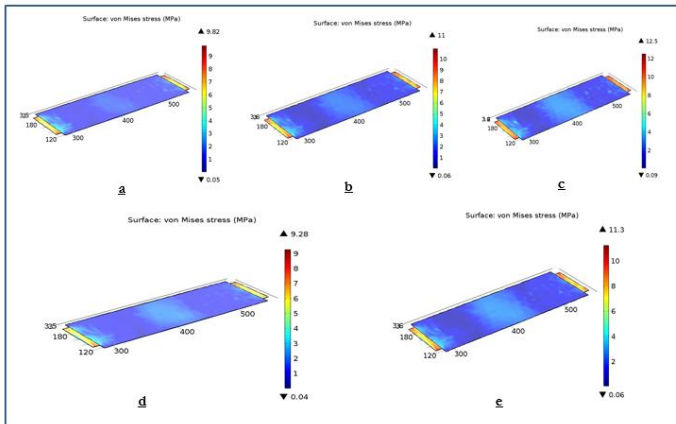


**Fig. 5.** Simulations of plane beam (Beam-1)

a) Aluminium b) Copper, c) Chromium, d) Gold, e) Platinum

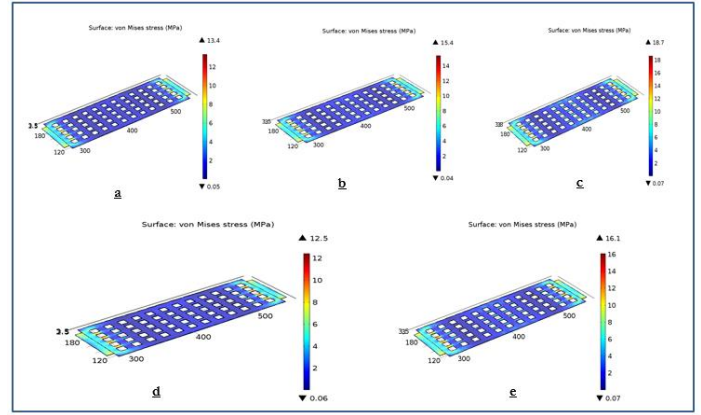


**Fig. 6.** Simulations results of beam with holes (Beam-2)

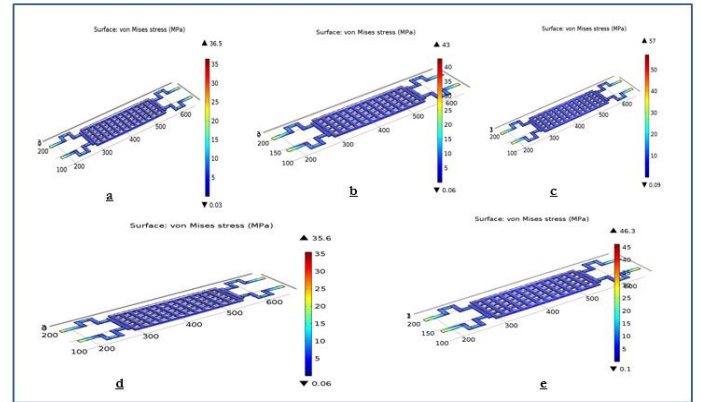


**Fig. 7.** Simulations analysis of beam with meanders and perforations (Beam-3)

Finally the proposed beam structure the stress is obtained as 35.6 MPa and a slope of 0.06 MPa/μm, the deformations of the beam were modelled for this extreme case is shown in above Figure 5, 6, and 7. (In all the figures gold beam is mentioned as (d)).

The maximum stress that happens with the length of beam and this stress is concentrated at the edges of the beam, as shown in Tables 3, 4 and, 5. Where the bridge structure connects to the supports and decreases towards the center of the membrane. It is understood that the fixed edges on the upper surface of the membrane are stretched and on the lower surface of the membrane are compressed.

**Table 3.** Stress analysis of beam with 0.5  $\mu\text{m}$  thickness

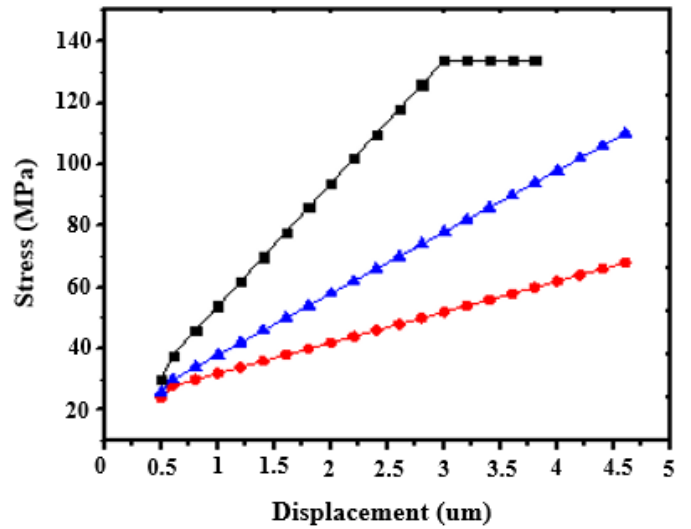
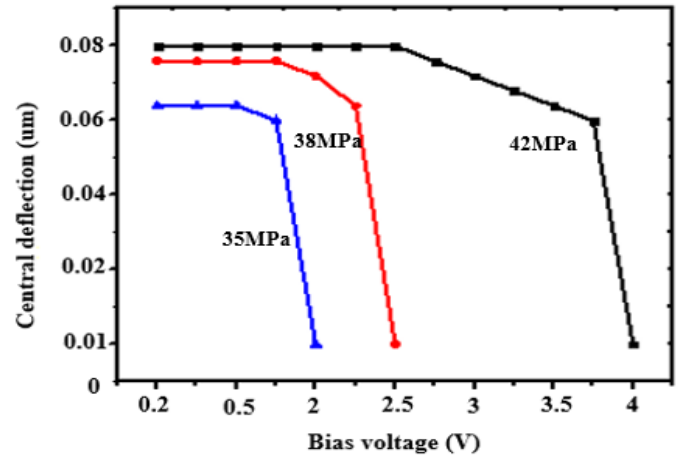
Materials	Stress (MPa) thickness @ 0.5 $\mu\text{m}$		
	Beam-1 (Plane beam)	Beam-2 (Inserted holes)	Beam-3(Added Holes and Meanders)
Aluminium (Al)	9.82	13.4	36.5
Copper (Cu)	11	15.4	43
Chromium (Cr)	12.5	18.7	57
Gold (Au)	9.28	12.5	35.6
Platinum (Pt)	11.3	16.1	46.3

**Table 4.** Stress analysis of beam with 1.5  $\mu\text{m}$  thickness

Materials	Stress (MPa) thickness @ 1.5 $\mu\text{m}$		
	Beam-1 (Plane beam)	Beam-2 (Inserted holes)	Beam-3(Added Holes and Meanders)
Aluminium (Al)	12.7	15	38.2
Copper (Cu)	14.26	17.2	45
Chromium (Cr)	15.7	21	59
Gold (Au)	11	15	38
Platinum (Pt)	13.9	18	49

**Table 5.** Stress analysis of beam with 2.5  $\mu\text{m}$  thickness

Materials	Stress (MPa) thickness @ 2.5 $\mu\text{m}$		
	Beam-1 (Plane beam)	Beam-2 (Inserted holes)	Beam-3(Added Holes and Meanders)
Aluminium (Al)	18.4	19	46
Copper (Cu)	20	21	48
Chromium(Cr)	19.2	24	64
Gold (Au)	17	20	42
Platinum (Pt)	19.6	22	61

**Fig. 8.** Minimum deflection of proposed switch along with the stress**Fig. 9.** Center deflections of proposed switch with gold material

The curves of the middle deflection of the stressed membrane versus the applied voltage predicted by the analyses are shown in Fig.8 and 9.

**Table 6.** Comparison results of proposed device with existing work

Parameters	Ref (T. Singh.et.al.2013)	Ref (Y. Mafinejad.et.al.2017)	Ref (Ansari.et.al.2020)	Proposed switch
Pull-in Voltage	8.2	18 and 25	9.2 V	1.9 V
Stress (MPa)	43.7	15-25	25	35.6
Materials	Aluminium (Al)	-----	-----	Gold (Au)

## 4 Conclusions

In this paper, the Electrostatic-mechanical model for fixed-fixed beam designs are presented. The stress analysis of different beam structures of RF MEMS Capacitive type switch is designed and simulated with perforations and non-uniform meanders. These are helps to reduce the squeeze film damping and stiction problems, these simulations are analysed in the COMSOL tool. The material properties are vital role by considering the beam for getting good performance of the device. We have taken different beam materials such as aluminium, copper, chromium, platinum, and gold, in all of these the gold has got good results. The actuation voltage of proposed switch is obtained as 1.9 V, the stress energy for a beam with a center deflection of 0.06 MPa/ $\mu\text{m}$  and an applied biaxial tensile stress of 35.6 MPa exceeds the critical value of gold (Au) in the absence of an actuated structure by an affected biaxial tensile stress, the significant positions are located near sharp corners at the fixed edges. During the simulation, we have observed that the switch closing voltage is not sensitive to stress, which makes it possible to manufacture a switch from metals at a low cost and high stress.

## Acknowledgement

The Authors are thankful to National MEMS Design Centre, NIT Silchar, Assam for providing essential Finite Element Modelling tools.

## References

- [1] Jaafar, Haslina, et al. "A comprehensive study on RF MEMS switch." *Microsystem Technologies* 20.12 (2014): 2109-2121.
- [2] Rebeiz, Gabriel M. "RF MEMS-theory, design, and technology." *John Wiley & Sons*, 2004.
- [3] Katehi, Linda PB, James F. Harvey, and Elliott Brown. "MEMS and Si micromachined circuits for high-frequency applications." *IEEE Transactions on Microwave Theory and Techniques* 50.3 (2002): 858-866.
- [4] Mafinejad, Yasser, et al. "Low insertion loss and high isolation capacitive RF MEMS switch with low pull-in voltage." *The International Journal of Advanced Manufacturing Technology* 93.1 (2017): 661-670.
- [5] Shojaei-Asanjan, Desireh, Maher Bakri-Kassem, and Raafat R. Mansour. "Analysis of thermally actuated RF-MEMS switches for power limiter applications." *Journal of Microelectromechanical Systems* 28.1 (2019): 107-113.
- [6] Philippine, Mandy A., et al. "Topology optimization of stressed capacitive RF MEMS switches." *Journal of microelectromechanical systems* 22.1 (2012): 206-215.
- [7] Shekhar, Sudhanshu, K. J. Vinoy, and G. K. Ananthasuresh. "Low-voltage high-reliability MEMS switch for millimeter wave 5G applications." *Journal of Micromechanics and Microengineering* 28.7 (2018): 075012.
- [8] Chakraborty, Amrita, Bhaskar Gupta, and Binay Kumar Sarkar. "Design, fabrication and characterization of miniature RF MEMS switched capacitor based phase shifter." *Microelectronics Journal* 45.8 (2014): 1093-1102.
- [9] Koutsourelis, M., et al. "Electrical properties of nanostructured SiN films for MEMS capacitive switches." *Journal of Micromechanics and Microengineering* 27.1 (2016): 014001.
- [10] Bansal, Deepak, et al. "Low voltage driven RF MEMS capacitive switch using reinforcement for reduced buckling." *Journal of Micromechanics and Microengineering* 27.2 (2016): 024001.
- [11] Subramanian, M. Bala, et al. "Multiport RF MEMS switch for satellite payload applications." *Microsystem Technologies* 24.5 (2018): 2379-2387.
- [12] Kumar, P. Ashok, K. Srinivasa Rao, and K. Girija Sravani. "Design and simulation of millimeter wave reconfigurable antenna using iterative meandered RF MEMS switch for 5G mobile communications." *Microsystem Technologies* (2019): 1-11.

- [13] Molaei, Somayye, and Bahram Azizollah Ganji. "Design and simulation of a novel RF MEMS shunt capacitive switch with low actuation voltage and high isolation." *Microsystem Technologies* 23.6 (2017): 1907-1912.
- [14] Sravani, K. Girija, and K. Srinivasa Rao. "Analysis of RF MEMS shunt capacitive switch with uniform and non-uniform meanders." *Microsystem Technologies* 24.2 (2018): 1309-1315.
- [15] Chu, Chenlei, Xiaoping Liao, and Hao Yan. "Ka-band RF MEMS capacitive switch with low loss, high isolation, long-term reliability and high power handling based on GaAs MMIC technology." *IET Microwaves, Antennas & Propagation* 11, no. 6 (2017): 942-948.
- [16] Rao, K. Srinivasa, P. Naveena, and K. Girija Sravani. "Materials Impact on the Performance Analysis and Optimization of RF MEMS Switch for 5G Reconfigurable Antenna." *Transactions on Electrical and Electronic Materials* 20, no. 4 (2019): 315-327.
- [17] Ansari, Hamid Reza, and Saeed Khosroabadi. "Design and simulation of a novel RF MEMS shunt capacitive switch with a unique spring for Ka-band application." *Microsystem Technologies* 25, no. 2 (2019): 531-540.
- [18] Singh, Tejinder, Navjot K. Khaira, and Jitendra S. Sengar. "Stress analysis using finite element modeling of a novel RF microelectromechanical system shunt switch designed on quartz substrate for low-voltage applications." *Transactions on electrical and electronic materials* 14.5 (2013): 225-230.
- [19] Dutta, Shankar, et al. "Effect of residual stress on RF MEMS switch." *Microsystem technologies* 17.12 (2011): 1739-1745.
- [20] Song, Yo-Tak, Hai-Young Lee, and Masayoshi Esashi. "Low Actuation Voltage Capacitive Shunt RF-MEMS Switch Using a Corrugated Bridge with HRS MEMS Package." *Journal of electromagnetic engineering and science* 6.2 (2006): 135-145.
- [21] Ansari, Hamid Reza, and Zoheir Kordrostami. "Development of a low stress RF MEMS double-cantilever shunt capacitive switch." *Microsystem Technologies* 26.8 (2020): 2739-2748.
- [22] Rao, K. Srinivasa, Lakshmi Narayana Thalluri, Koushik Guha, and K. Girija Sravani. "Fabrication and characterization of capacitive RF MEMS perforated switch." *IEEE Access* 6 (2018): 77519-77528
- [23] Solazzi, Francesco. "Novel design solutions for high reliability RF MEMS switches." PhD diss., University of Trento, 2011.
- [24] Rao, K. Srinivasa, Ch Gopi Chand, K. Girija Sravani, D. Prathyusha, P. Naveena, G. Sai Lakshmi, P. Ashok Kumar, and T. Lakshmi Narayana. "Design, modeling and analysis of perforated RF MEMS capacitive shunt switch." *IEEE Access* 7 (2019): 74869-74878.
- [25] Sravani, K. Girija, D. Prathyusha, K. Srinivasa Rao, P. Ashok Kumar, G. Sai Lakshmi, Ch Gopi Chand, P. Naveena, Lakshmi Narayana Thalluri, and Koushik Guha. "Design and Performance Analysis of Low Pull-In Voltage of Dimple Type Capacitive RF MEMS Shunt Switch for Ka-Band." *IEEE Access* 7 (2019): 44471-44488.